

## 3D physical modelling in a wave flume of brine discharges on a beach

F. Vila\*, A. Ruiz-Mateo, M. Rodrigo, A. Álvarez, M. Antequera, A. Lloret

Centre for Studies on Ports and Coasts of CEDEX. Madrid, Spain  
Tel. +34 (913) 357 722; Fax +34 (913) 357 601; email: francisco.vila@cedex.es

Received 16 August 2010; Accepted in revised form 6 April 2011

---

### ABSTRACT

The seawater desalination process is a strong bet for developing regions like the Spanish Mediterranean, to satisfy the increasing fresh water demand, or the Canary Islands, being the desalination the most important artificial water resource. The main characteristic of the waste brine disposal resulting from the desalination process is its high salinity, and consequently, its higher density in comparison with that of the environment. Therefore, the discharge of the concentrated effluent into the sea may cause a negative impact in the sea water quality and its ecosystems, specially regarding the sea grass meadows that cover the Mediterranean coast. In order to make the development of the desalination plants sustainable, the Spanish Ministry of the Environment and Rural and Marine Affairs agreed to invest in Experimental Development Projects within its National Plan for Scientific Research, Development and Technological Innovation. The project entitled "Development and implementation of a methodology to reduce the environmental impact of brine discharges from desalination" has been approved and supported as a part of the Plan. This project is being carried out by the University of Cantabria in collaboration with the Spanish Centre for Experimentation on Public Works (CEDEX). The aim of this study is to find which discharge devices produce the biggest brine dilution, to make the environmental impact on the biocenosis as low as possible. Under this perspective, the behaviour of different jets and discharge devices were investigated in physical models. To this purpose, different instrumentation has been using to measure the conductivity and velocity in the near and far field of the effluent, including a micro scale conductivity and temperature instrument or a doppler velocity profiler. Part of the experiments have been performing in a wave flume of 30 m long, 1 m wide and 2 m high, simulating a 3D superficial discharge from a beach with a fixed slope. In this flume different simulations, changing the wave variable (height and period, in an irregular JONSWAP train wave), have been testing. The results obtained with the performed physical model will be presented in this communication.

*Keywords:* Physical model; Brine disposal; Desalination; Dilution; Brine discharge device; Wave flume

---

### 1. Introduction

#### 1.1. Brine characteristics

Because of its magnitude, the most important waste disposal of a desalination plant is the water discharge.

An inverse osmosis desalination plant using marine water (conversion of 45%) with a production of 70,000 m<sup>3</sup>/d of desalted water will generate a discharge of 1 m<sup>3</sup>/s. If it is an inverse osmosis desalination plant using brackish water (conversion of 80%), it will generate a discharge of 0.2 m<sup>3</sup>/s and in the case it is a distillation plant (conversion 10%) it will produce a discharge of 7.3 m<sup>3</sup>/s.

\* Corresponding author.

At the beginning it was assumed that the components of the discharged waters due to the substances ported by the source water were the least worrisomely, specially when the discharge is produced in the same medium from where the source water is collected (this happens when we extract source water from sea) because there is no addition of contaminants to the system.

When the total gross water is taken from the sea and the discharge is driven back to this medium, salinity will increase 70% if we are dealing with an inverse osmosis plant. If the discharge is done in a non-vegetated area, there will not be much problem, but if in the vicinity there are communities of biological interest because of their productivity, biodiversity or rareness, the possible effects of the increment in salinity must be studied and decide if this increase is acceptable before authorising the discharge. In any case, the design of a discharge device that produces a strong dilution in a small space (mixing zone) will make it easier to find an appropriate point of discharge without going beyond the limits of tolerance of these biological communities.

### 1.2. Brine behaviour when it is discharged into the sea

When the effluent reaches the sea, its kinetic energy creates turbulences that produce a fast partial mixture with the receiving waters, even when these waters are in calm (near field). Also, if the discharge is done far away from the bottom or if it is done in such a way that several jets are formed in opposite direction to the bottom, the potential energy produced due to the mayor density of the discharged water also contributes to the turbulence effect created. Of course, the intensity of this mixing, and therefore the dilution obtained in the near-field will increase with the kinetic energy of the effluent, the kinetic energy of the receiving waters (waves) and with the area of contact between both in the turbulence area. The initial dilution obtained with a multiport diffuser with several thin jets with enough separation between them, will always be greater than a discharge with a single open channel with or without spillway, although the hydraulic load necessary will also have to be greater.

In any case, at certain distance of the discharge device the turbulence is attenuated and the mixing, with a better or worse dilution, ends forming a layer generally hyperdense<sup>1</sup> that flows, spreading out, over the bottom. As the fluid advance, its width grows due to the lateral spreading (if it is not channelled) and consequently, its thickness decreases. At the same time, a slow but inexorable mixing between the hyperdense layer and the ambient water

takes place, which causes the appearance and continuous increase of an interface layer with intermediate salinities between the former layers. The thickness is getting reduced until it becomes almost indistinguishable from the environmental waters.

When the hiperdense layer is highly dilute, if the receiving waters are naturally stratified because of the temperature gradient (water is cooler at the bottom), this layer leave the bottom and flow between two different layers with a intermediate density between the bottom and the surface one.

### 1.3. Environmental impact. Threshold of tolerance

The effect that the brine discharge causes on marine organisms is still unknown [1]. Although several highly specialized sectorial studies can be found among the scientist literature, they are usually focus on determine the effect of a specific pollutant in a specific specie and even then, conclusive results are not always presented.

An example of one of these sectorial studies was the determination of the threshold of tolerance of the endemic Mediterranean seagrass, *Posidonia oceanica*<sup>2</sup>, which covers the infralitoral zone of the Mediterranean coast as a continuous meadow. As a result of the study it was concluded that this specie has narrow threshold of tolerant, around 1 g/kg of salinity increase [2].

### 1.4. A methodology for the design of brine discharges into the seawater. MEDVSA project

The design of the discharged of the hiperdense effluent generated during the desalination process is nowadays one of the most important and sometimes one of the most difficult troubles which need to be solved within any desalination plant construction project.

These troubles arise from the strict security margin imposed due to the lack of contrasted data of the negative effects of brine discharges more than from technical difficulties to obtain the necessary dilution to protect the marine ecosystems. The Desalination Committee of the American Water Works Association (AWWA) published in 2004 Water Desalting Planning Guides [3] in which it was stated

*Regulations pertaining to concentrate discharge are complex and stringent. In some situations concentrate disposal costs and other disposal issues are so significant that they determine the overall feasibility of a desalting project. As such, concentrate disposal is a key consideration for any desalting project.*

<sup>1</sup> If the desalination plant has a low conversion factor, the effluent may have less density than the seawater. In this case it is formed a hipodense layer that spreads over the sea surface. This behaviour is also observed whit thermal desalination plants or when the brine effluent is previously mixed with the effluent resulted from a wastewater treatment plant.

<sup>2</sup> The *Posidonia oceanica* meadows are included in Annex I (natural habitat types of community interest whose conservation requires the designation of special areas of conservation) of the Council Directive 92/43/EEC of 21 May 1992 on the conservation of natural habitats and of wild fauna and flora. It is also marked as a priority habitat type.

In order to palliate the water deficit suffered in the Southeast of Spain and the Canary Islands, the desalination plants have been rapidly implanted along the Mediterranean coast. At the same time, the start up of the current Spanish National Hydrologic Plan, has contributed to increase the sea water desalination demand as the main fresh water source supply, which implies the rise in the brine flow discharged into the sea.

Nowadays, it does not exist either legal legislation which regulates brine discharges into the sea or any methodological tool for the discharge designing optimization. For this reason, promoters and the administrative responsible, in several occasions do not apply common criteria to assure the protection of the marine environment from this kind of discharges. Since the year 2000, CEDEX is working following in the footsteps of solving the mentioned lack of information of brine behaviour. It has carried out several studies [4] and technical papers [5] with the aim of optimizing the design as well as minimizing the negatives impacts on marine ecosystems.

Taking in mind this situation, the Research and Development (R&D) project “MEDVSA Development and implementation of a Methodology to reduce the brine discharge environmental impact”, financed by the Spanish Ministry of the Environment and Rural and Marine Affairs, is conceived with the aim of offering a methodology which includes all the technical and environmental features for a correct brine discharge management, taking into account the Mediterranean coasts particularities. Two important Spanish Research Centres in coastal and environment engineering matters are collaborating in “MEDVSA” project: the Environmental Hydraulics Institute “IH Cantabria” of the University of Cantabria, and the Centre of Studies and Experimentation of Public Works (CEDEX) of the Ministry of Public Works [6].

The main objective of the project is to make compatible the use of desalination as an important water resource in some Spanish coastal areas, with the environmental

protection of the marine areas, while following sustainable development principles.

To achieve the overall objective, it was raised the following specific objectives from a scientific and technological point of view.

- Optimizing systems and criteria in the discharges into the sea of the brine produced in Spanish desalination plants. This entails to perform experimental testing in reduced physical model, development and calibration of numerical modelling tools for simulating the phenomenon and validation of these tools with data from discharges of desalination plants in operation.
- Developing a general methodology for carrying out studies, which take into account all the aspects to be considered: location of the spill; the most appropriate system discharge; methodology or criteria for characterization of effluent and the receiving environment in each case; numerical modelling of the phenomenon; environmental quality standards in the receiving environment depending on the type of existing ecosystems and establishment of environmental monitoring plans, among others.

Among the different tasks considered in the project one of the most important is the “Experimental analysis of different discharge devices”. Actually, there are several kinds of discharge devices. The most representative of desalination plants placed in Spain were selected:

- Discharge from a beach
- Discharge from overflow spillway in a cliff
- Discharge from a submerge outfall
- Discharge from a breakwater

The present work shows the experimental analysis carried out for CEDEX to study the brine discharge from a beach. In Spain, the kind of discharging through superficial devices can be observed in some desalination plants. Figs. 1–3 show a few examples.



Fig. 1. Sureste (Gran Canaria) desalination plant discharge.



Fig. 2. Alicante I and Alicante II desalination plant discharge.



Fig. 3. Palma de Mallorca desalination plant discharge.

## 2. Theoretical analysis. Approach to the problem

For the numerical analysis of the problem, the brine discharge is treated as a hyperdense discharge with density  $\rho + \Delta\rho$  for a homogeneous environment of density  $\rho$ . As it was previously discussed and it is already known, the surface discharge, denser than the ambient, will become a submerged density current [7], with a transition from the surface current to the submerged [8]. Therefore, the discharge enters to the environment through-out the entire water column. This occupation will continue in the space until the negative buoyancy is imposed to the initial momentum of the discharge. At that point the discharge will be submerged, becoming a density current (Fig. 4).

Then the independent variables to consider in the problem are shown in Fig. 5.

- $Q_0 = A \cdot u_0$
- $M_0 = u_0 \cdot Q_0$
- $G_0 = g'_0 \cdot Q_0$
- $x$
- $y$
- $B_0$  ( $o e_0$ )

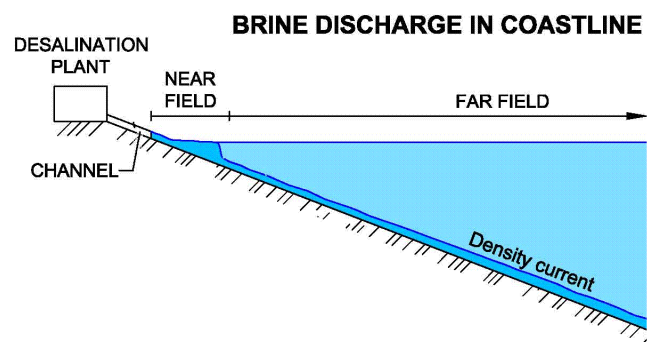


Fig. 4. Surface discharge device.

Therefore there are six independent variables of which only there are two independent dimensions (length and time, the mass is removed by considering only the  $g'$  as representative of the mass implied). The dimensional analysis shows that we have four degrees of freedom, i.e. it is possible to build four dimensionless monomials or to generate five monomials with a single dimension.

- $Q_0 = A \cdot u_0$
- $M_0 = u_0 \cdot Q_0$
- $G_0 = g'_0 \cdot Q_0$
- $x$
- $y$
- $B_0$  ( $o e_0$ )

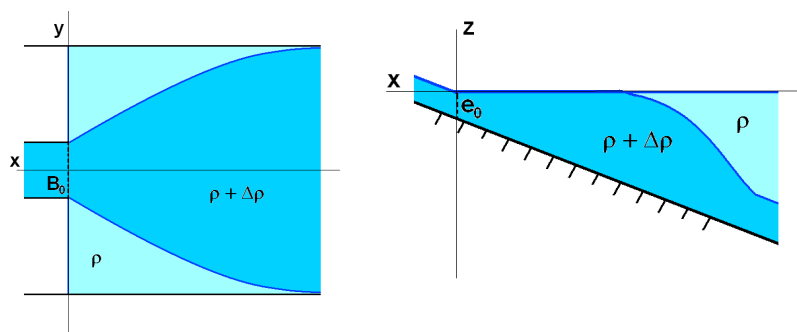


Diagram of discharge variables (Left: elevation. Right: profile)

Fig. 5. independent variables.

The first option (dimensionless) could be:

- $L_{MG}/L_{QM} = u_0 \cdot g'_0{}^{-1/2} \cdot A^{-1/4} = F_{d0}$
- $x/L_{QM}$
- $y/L_{QM}$
- $B_0/L_{QM}$

The second option (dimension length) could be:

- $L_{QM} = Q_0 \cdot M_0^{-1/2}$
- $L_{MG} = M_0^{3/4} \cdot G_0^{-1/2}$
- $x$
- $y$
- $B_0$

However in the case of a surface discharge, an asymptotic approach can be performed without making excessive errors: it is assumed that the initial momentum ( $M_0$  or  $u_0$ ) tends quickly to zero. Therefore if the variable  $M_0$  is neglected, the problem will arise from the variables  $x$ ,  $y$ ,  $Q_0$ ,  $G_0$  and  $B_0$ . So now, there are three dimensionless monomials:

- $x/L_{QG}$
- $y/L_{QG}$
- $B_0/L_{QG} = 1/F_d^{2/5}$  where  $F_{d,B0} = Q_0 \cdot (G_0 \cdot B_{05})^{-1/2}$

or four monomials with dimension of length:

- $L_{QG} = Q_0^{3/5} \cdot G_0^{-1/5}$
- $x$
- $y$
- $B_0$

On other hand, the dilution  $D$  is usually defined as the ratio of the total sample volume ( $V$ ) and the volume of effluent contained in that sample ( $V_0$ ):

$$D = \frac{V}{V_0} \tag{1}$$

On the basis of dimensional analysis, it can be affirmed that any dimensionless dependent variable (it is mean dimensionless using the independent variables) can be

expressed as a function of dimensionless variables written above [9]. For example, the dilution at a given point, which is a dimensionless variable, can be expressed:

$$D = f\left(\frac{x}{L_{QG}}, \frac{y}{L_{QG}}, \frac{B_0}{L_{QG}}\right) \tag{2}$$

If the effluent has a concentration of salt  $S_0$  and the salt is also present in environmental water with a concentration  $S_a$ , then the concentration of salt of the sample is:

$$\begin{aligned} S &= \frac{m}{V} = \frac{m_0 + m_a}{V} = \frac{S_0 \cdot V_0 + S_a \cdot (D-1) \cdot V_0}{D \cdot V_0} \\ &= \frac{S_0 + S_a \cdot (D-1)}{D} \end{aligned} \tag{3}$$

That could be given as:

$$s - s_a = \frac{s_0 - s_a}{D} \tag{4}$$

Solving the equation, the dilution can be calculated by dividing the two differences:

$$D = \frac{s_0 - s_a}{s - s_a} \tag{5}$$

So returning to Eq. (2), the salinity at any point in the physical model can take an expression that is dependent function of the dimensionless variables ( $x/L_{QG}$ ,  $y/L_{QG}$ ,  $B_0/L_{QG}$ ):

$$\frac{s_0 - s_a}{s - s_a} = f\left(\frac{x}{L_{QG}}, \frac{y}{L_{QG}}, \frac{B_0}{L_{QG}}\right) \tag{6}$$

For the treatment of the results, it was found more intuitive to work with the percentage remaining discharge ( $D^{-1}(\%)$ ) which is defined as:

$$D^{-1}(\%) = \frac{100}{D} = 100 \cdot \left(\frac{s - s_a}{s_0 - s_a}\right) \tag{7}$$

That has the advantage that its value is always between 0 (water of the environment) and 100 (undiluted effluent).

### 3. Physical model

The Centre for Studies on Ports and Coasts of CEDEX has an extensive experience in developing physical models of brine discharges into the sea [10]. Among the facilities it has, the concern of this article is the wave flume with 70 m long, 1 m wide and 1.5 m high. This wave flume was divided by two. Using 40 m of it, a physical model was designed to represent a beach profile as follows (Figs. 6 and 7):

- The first 3 m, 10% slope.
- The following 5.5 m, variable slope with a Bruun typical profile:  $h(x) = 0.25 x^{2/3}$
- The following meters, up to 30 m away from the discharge point, 2% slope.

Fig. 6 shows the built beach profile.

At the far end of the discharge point of the model, the flume has a wave generator (Fig. 8) which was used to reproduce several typical marine conditions on the Spanish coast.

To take advantage of the wide flume to simulate the 3D

behaviour, the discharge was performed by attaching it to one wall of the channel (Fig. 9). Taking this wall as a vertical plane of symmetry of the discharge, the results may be extended to twice the width of the channel.

In the case of physical model tests, the water of the receiving environment has much lower salinity than the one sea water (in fact  $S_a \approx 0$  psu). Thus, to simulate the conditions similar to the real ones, the discharge which simulates the brine of the desalination plant, was modified accordingly in order to maintain the similarity of the Froude densimetric<sup>3</sup> number of the prototype to the model. Therefore, it was sought that the relationship,  $\Delta\rho \cdot \rho^{-1}$ , between the effluent and the receiving water were the same in the physical model and in the prototype. So that, if it is considered a desalination plant with an effluent density  $\rho_0$  (determined by a salinity  $S_0$  and a temperature  $T_0^\circ$ ) that pour to a receiving environment with a density  $\rho_a$  (determined by a salinity  $S_a$  and a temperature  $T_a^\circ$ ) a specific<sup>4</sup> relationship  $\Delta\rho \cdot \rho^{-1}$  can be obtained. Based

<sup>3</sup> The Froude number is a dimensionless number relating the inertial to gravity forces acting on the fluid. Together with the acceleration of the gravity and the length, it is an independent vector basis which is fixed to transform the rest of the magnitudes from a prototype to a model.

<sup>4</sup> An example of a desalination plant would be one of a con-

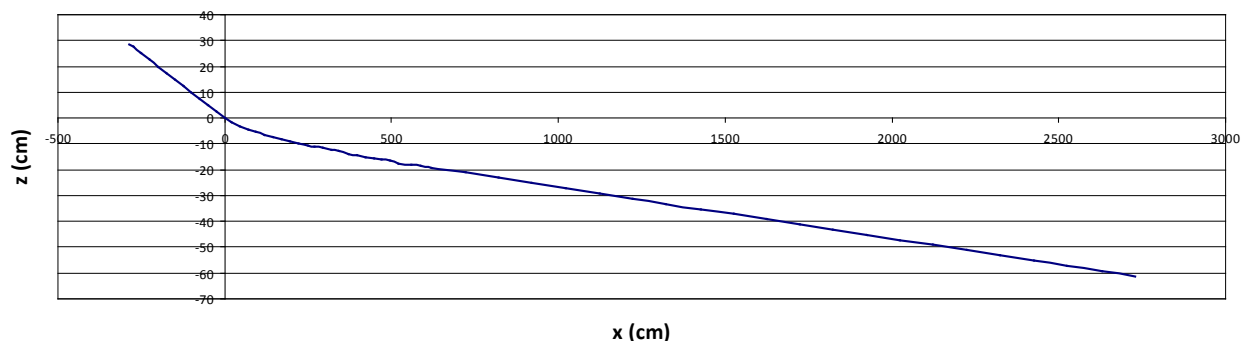


Fig. 6. Built beach profile in the wave flume.



Fig. 7. Wave flume in the Centre for Harbours and Coastal Studies of CEDEX.



Fig. 8. Wave generator. Control booth of the wave generator.



Fig. 9. Flume of the discharge attached to the wall.



on this condition and on the environment conditions of the experiment, temperature of the receiving environment and the discharge (it varies in winter time at temperatures of 10°C and in summer at temperatures of 20°C) and salinity of the receiving environment, the salinity of the discharge is adjusted by adding salt (NaCl) to a greater or lesser amount.

The discharge is stained with rhodamine WT, which is used to keep track and provide some measurements during the experiment (thick hyperdense layer or plunged point, Fig. 10).

The effluent is channelled before reaching the environment and. A gate is placed (Fig. 11) to control the output speed and it generates a section that involves a specific speed at a flow set in advance.

The tests are performed varying certain characteristics of the discharge: the input velocity to the discharge en-

vironment, the width of the discharge and the discharge flow. At the same time, several tests are carried out by changing the environment swell conditions: calm, low swell, moderate swell and heavy swell.

The mean sea level is not changed from one test to another. To avoid the impact of waves on the gate (run-up), it is delayed according to the wave intensity (Fig. 12).

Since reached speed was higher than the expected when the discharge was channelled down a slope of 10% – even the reached speed was so high that translated to a real scale it involves an excessive speed for a discharge – it was decided to halt the discharge and to generate a subcritical flow which allowed to handle the output seed. This was achieved by setting one or two tablets just before the gate (Fig. 12).

After fixing the height of the gate, the resulting section was photographed. Subsequently the experiment, with the help of an image processing program, the area was determined with high accuracy by determining the output speed of the discharge.

It was decided to use a length scale of 1:16 for the test. This scale and the condition of similarity of Froude

---

version factor of 50% to produce a discharge of 68.2 psu salinity and temperature of 18°C. With a receiving medium salinity of 37.5 psu at  $T = 20^\circ\text{C}$ , it obtains a relationship  $\Delta\rho \cdot \rho^{-1} = 0,0227514$ .



Fig. 10. Because of the rhodamine stained, it can be estimated the plunged area (left) or the thickness of the hyperdense layer (right).

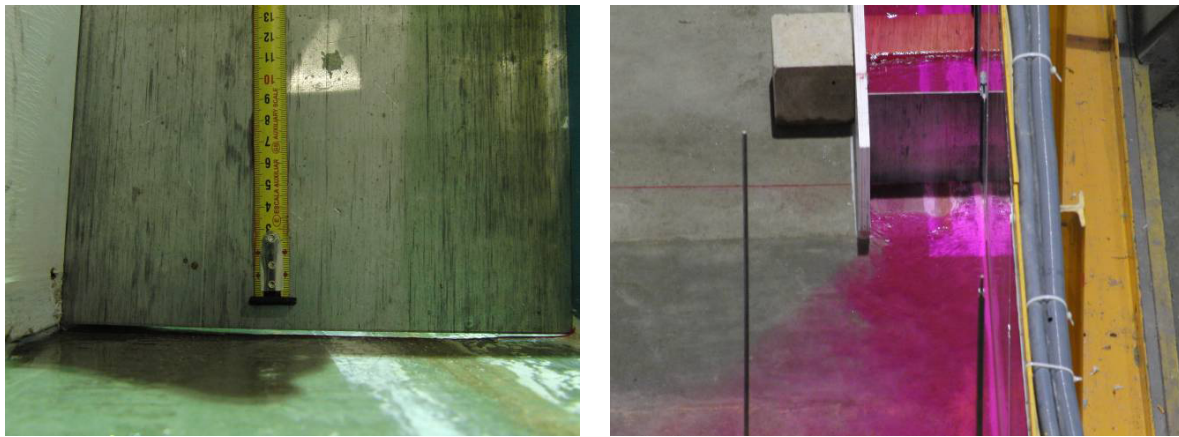


Fig. 11. Output gate which fix the input velocity of the discharge to the environment.

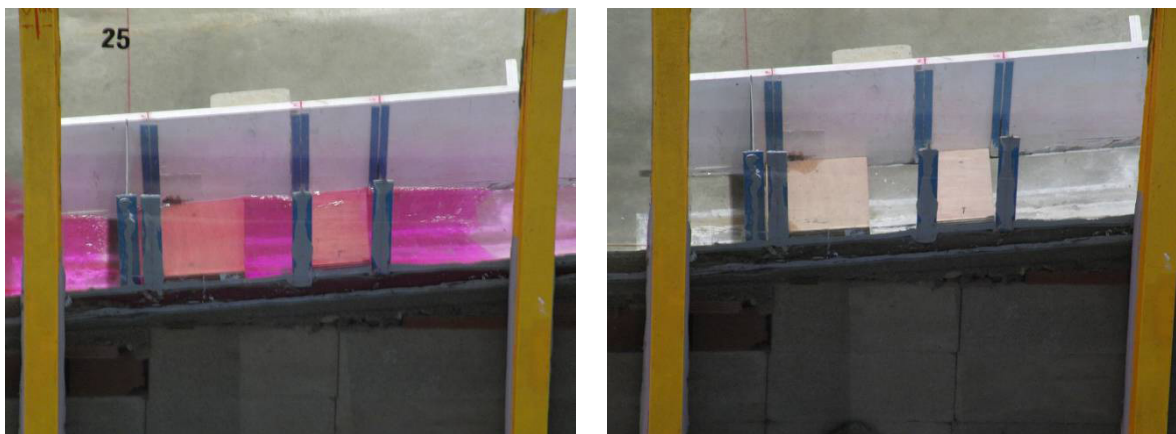


Fig. 12. The blue vertical stripes show the position where the gate is placed according to the intensity of the waves. The figure show, also, the tablets to stop the discharge.

determine both the width of the flume (6 cm) as well as de flow (23.4 l/min) on which to start the tests. Likewise, the scale transforms: the output speeds of the discharge, height and period wave (see next section: swell).

Because of the very high flow it was needed to prepare a large volume of brine prior to test. Also, it entails the difficulty that the pumps, that drive the discharge from storage tanks to the test flume, have different working





Fig. 13. The discharge storage tanks.



Fig. 14. System to prevent flow fluctuations due to variations in the water column over the pumps work.

conditions by varying the liquid level of storage tanks therefore, the initial flow varies. The way to overcome these two difficulties was connecting two storage tanks of 2500 l each (Fig. 13) on which the discharge was generated. With 5000 l for a flow of 23.4 l/min gives 3.5 h of testing, about 4 tests.

The second difficulty was solved thanks to two facts: the connection of the two tanks (Fig. 13), which causes, through the effect of “communicating vessels”, the pressure of the water column varies slowly (Fig. 14); and the installation of a constant flow device (Fig. 14), which prevents variations and fluctuations in the final fluid.

The hydraulic system is a set of keys including flow control and security, in case of breakage or bad operation.

### 3.1. Swell

For the generation of waves, the software “GEDAP WAVE GENERATION SOFTWARE”, Canadian Hydraulics Centre [11] was used. Three irregular wave trains were generated according to a JONSWAP Spectrum for  $\gamma = 3.3$ , with different magnitudes, scaled to 1:16 (Table 1).

Higher waves were not performed because, in such cases, the dilutions are always above the minimum required.

### 3.2. Instrumentation

The tests were performed using the following instrumentation:

*Pipettes – peristaltic pumps:* through silicone tubes attached to a Pasteur pipette, it sucks up liquid sample to measure the conductivity and the temperature in the laboratory. 12 sets of pipettes, clustered in groups of three, were placed. Each set of pipettes has 4–6 tubes and it takes points in the same vertical profile separated 1 cm each. Each group of three sets of pipettes were placed in the same cross section (one attached to each side wall and one in the centre). They were connected to a separated peristaltic pump, positioned at a given distance (varying from one test to another) from the discharge point.

*Micro scale conductivity and temperature instrument (MSCTi):* it is sampled at a point with a resolution of 3 mm. It get sample with a frequency of up to 50 Hz, appropriate for measuring turbulence and wave effects on discharge. The tests were performed at a frequency of 20 Hz. The MSCTi, measuring during the test, was placed next to a given pipette to compare both results.

*Ultrasonic profiler velocity doppler (UPV):* it performs velocity profiles and it can measure distances greater than 60 cm with high resolution. It is necessary a good seeding of particles to reflect the ultrasonic beam. In the tests it is used at particular times and near to a set of pipettes.

Table 1  
Scaling types of irregular waves in physical models

Irregular swell JONSWAP ( $\gamma = 3.3$ )	Significant height ( $H_s$ )		Peak period ( $T_p$ )	
	Prototype	Model (1:16)	Prototype	Model (1:16)
Low swell	0.2 m	1.25 cm	4 s	1 s
Moderate swell	0.6 m	3.75 cm	6 s	1.5 s
Heavy swell	1.8 m	11.25cm	10 s	2.5 s



Fig. 15. Wave types: left: low; middle: moderate; right: heavy.

Table 2  
Test at the Centre for Harbours and Coastal Studies of CEDEX under MEDVSA Project

$H_s$ (cm)	$T_p$ (s)	$Q$ (l/min)	$h_0$ (mm)	$B_0$ (cm)	Froude, h	Froude, B
0	0	23.4	15	6	7.3	0.92
1.25	1	23.4	15	6	7.3	0.92
3.75	1.5	23.4	15	6	7.3	0.92
11.25	2.5	23.4	15	6	7.3	0.92
3.5*	1.5*	23.4	15	6	7.3	0.92
11.25*	2.5*	23.4	15	6	7.3	0.92
Mixto*	Mixto*	23.4	15	6	7.3	0.92
0	0	23.4	9	6	15.8	0.92
0	0	23.4	5.9	6	29.8	0.92
0	0	49.9	15	6	15.7	1.96
0	0	23.4	9	24	15.7	0.03
1.25	1	23.4	9	24	15.7	0.03
3.75	1.5	23.4	9	24	15.7	0.03

\* Regular swell. Mixed: during part of the test there was no swell. Then, regular swell with  $H_s = 3.5$  cm and  $T_p = 1$  s.



Fig. 16. Pasteur pipettes and peristaltic pump taking out liquid during a test.



Fig. 17. MSCTi and several devices involved in their use.

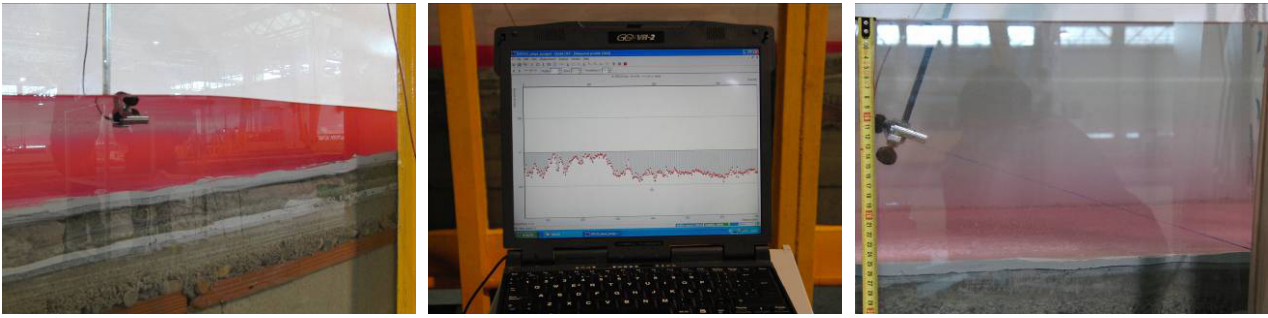


Fig. 18. UPV in operation and the signal during a measurement performed.

#### 4. Results

Four different types of studies, relating to surface discharge on the beach, were performed:

- Analysis of the influence of waves on the dilution of the discharge.
- Analysis of the influence of flow on the dilution of the discharge.
- Analysis of the influence of the flow thickness on dilution.
- Analysis of the influence of the flow width on dilution.

This paper only deals the influence of waves on the discharge. The following items were researched in performed test:

- Dilution of the discharge at different distances
- Hyperdense layer thickness
- Plunged point
- Progress velocity and hyperdense layer velocity
- Sequential analysis of salinity fluctuations in time (irregular waves vs. regular waves)

##### 4.1. Study of the dilution and its relation with the plunged point

For the dilution study, 10 different tests were performed varying only the magnitude of the wave for two different initial conditions of discharge (Table 2 and Table 3).

The first test was conducted under calm conditions. Under these conditions, without any turbulence, it is expected to present a very low dilution, being the worst condition to spill. According to performed tests, this is not true. Indeed, performed tests, for some wave conditions, provide results with worse dilution result than calm condition test. In the test, the dilution increase only with heavy wave condition.

Figs. 19–22 were made from the results obtained by extracting a sample volume, representing different sections of the flume for each type of test. In the figures, the red circles are points of sample extracted and the interpolated lines correspond to the percentage remaining discharge [ $D^{-1}(\%)$ ]. For the cases of calm condition (Fig. 19) and low swell condition (Fig. 20), the differences in dilution are

very small, almost negligible, probably because of the waves are too small to generate any kind of disturbance in the discharge. However, in the moderate swell case (Fig. 21), the dilutions are much lower ( $D^{-1}(\%)$  much higher), precisely for a swell which implies a significant turbulence in the surf zone, the dilution rather than better, are much lower (factor 2) than the dilution with calm conditions (Fig. 19).

From the CEDEX is working to explain this phenomenon (still having to rule out an scale effect due to the narrowness of the flume): In the performed tests are observed, including regular swell tests (see Figs. 23–25 and Table 3), that after the plunged zone the dilutions vary practically nothing or do it very slowly. Therefore, this implies that dilution process occur mostly in the area prior to the plunged [9]. Then, the study of this area appears to be essential [8].

If the geometry of the plunged zone is observed (depth and distance from the discharge), only in the heavy swell condition (Table 3) this area is enlarged compared to the area covered by the plunged zone in calm condition. This spreading is produced because of the turbulence generated by wave breaking. This plunged zone ranges due to irregular swell. In the other tests, this zone does not vary or becomes smaller in comparison to the calm condition.

Likewise, if the breaking point of the different tests is observed (Table 3), it shows that the heavy swell breaking point always lies outside the plunged point (compared to calm conditions) while in the other swell conditions the breaking points are produced within the plunged zone.

On this basis, it is concluded that in the case of heavy swell condition the breaking wave introduces clean water in the plunged zone favouring the dilution, while the other swell conditions do not introduce clean water because of its breaking points occur in the plunged zone, it reintroduces water with a big presence of discharge causing a re-concentration of the spill.

Furthermore, the tensor wave radiation was taken into account. This tensor causes a compression of the plunged area, reduces this area respect to calm conditions and slows the spill. Then if at the same time the breaking wave is reintroducing the spill in the plunged and compressed

Table 3  
Visual results of the test

Tests for this discharges conditions: $B_0 = 6 \text{ cm}; h_0 = 1.5 \text{ cm}; Q_0 = 23.4 \text{ l/min}$	Plunged point*		Breaking point ( $x/B_0$ )
	( $x/B_0$ )	( $z/h_0$ )	
Calm: $H_s = 0 \text{ cm}, T_p = 0 \text{ s}$	36.3	7	—
Low swell: $H_s = 1.25 \text{ cm}, T_p = 1 \text{ s}$	40.2	8	1–4
Moderate swell: $H_s = 3.75 \text{ cm}, T_p = 1.5 \text{ s}$	35.2–43.8	6.5–7.3	1–20
Heavy swell: $H_s = 11.25 \text{ cm}, T_p = 2.5 \text{ s}$	148–215.5	17.3–22.6	52.2–218.8
Moderate swell regular: $H = 3.5 \text{ cm}, T = 1.5 \text{ s}$	20.83	4.7	15.5
Heavy swell regular: $H = 11.25 \text{ cm}, T = 2.5 \text{ s}$	95–125.5	11.3–15.3	85.5–118.8
Mixed swell regular: $H = 0 \text{ cm}, T = 0 \text{ s}$	36.7	7	—
$H = 3.5 \text{ cm}, T = 1.5 \text{ s}$	20	5	15.5
Tests for this discharges conditions: $B_0 = 24 \text{ cm}; h_0 = 0.9 \text{ cm}; Q_0 = 23.4 \text{ l/min}$	Plunged point*		Breaking point
	( $x/B_0$ )	( $z/h_0$ )	( $x/B_0$ )
Calm: $H_s = 0 \text{ cm}, T_p = 0 \text{ s}$	3.2	6.1	—
Low swell: $H_s = 1.25 \text{ cm}, T_p = 1 \text{ s}$	2.83–3.3	5.5–6.1	0.25–1
Moderate swell: $H_s = 3.75 \text{ cm}, T_p = 1.5 \text{ s}$	6.8–11.3	10.3–13.9	0.25–5

\* In the irregular swell (and even regular) the “plunged point” is not a fixed point, therefore is better call it “plunged zone”, likewise the same happened when talking about “breaking point”, the “breaking zone” or the “surf zone”.

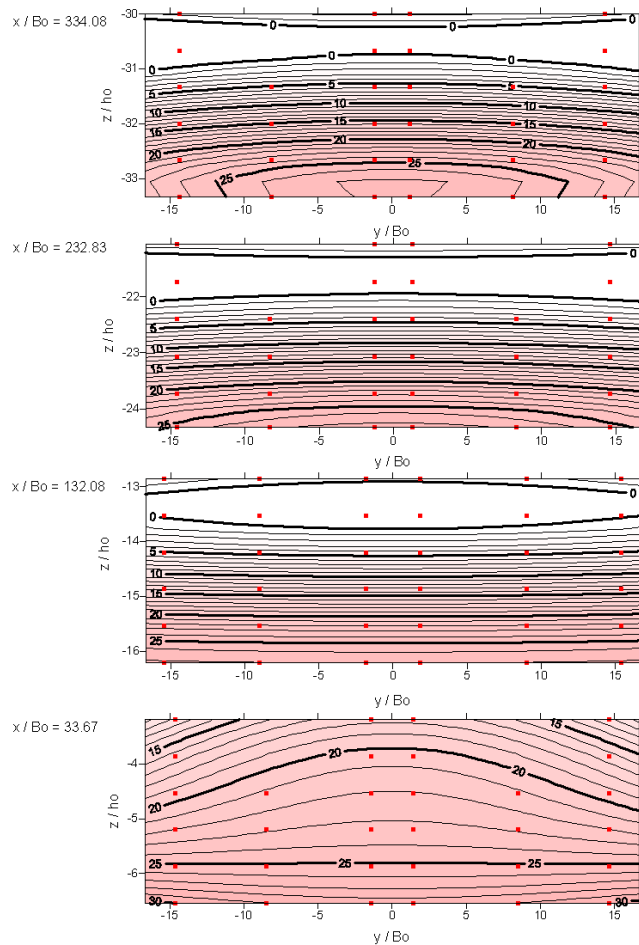


Fig. 19. Calm condition.  $B_0 = 6 \text{ cm}; h_0 = 1.5 \text{ cm}$ .

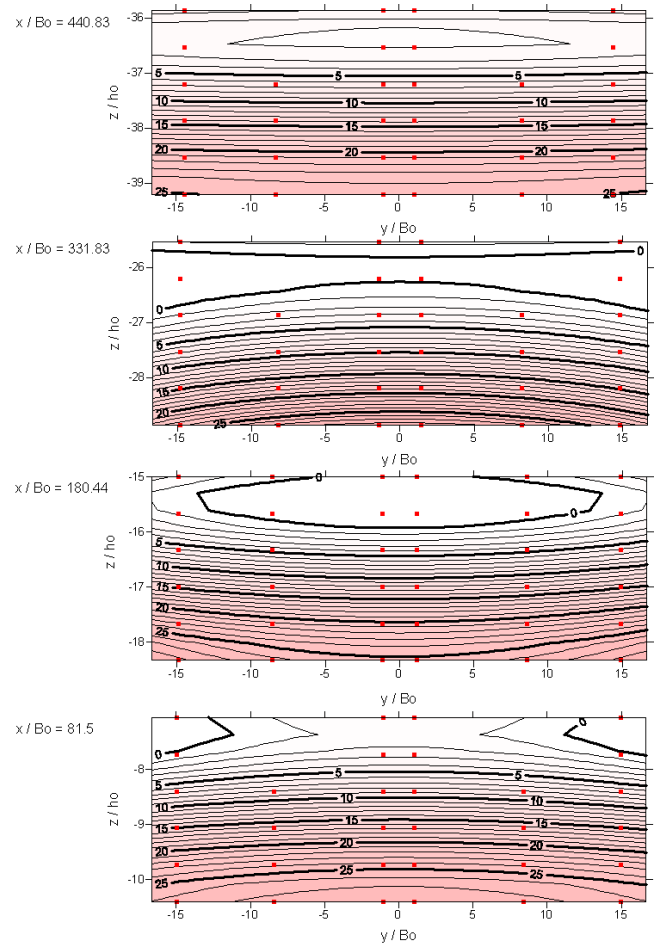


Fig. 20. Swell:  $H_s = 1.25 \text{ cm}, T_p = 1 \text{ s}, B_0 = 6 \text{ cm}, h_0 = 1.5 \text{ cm}$ .

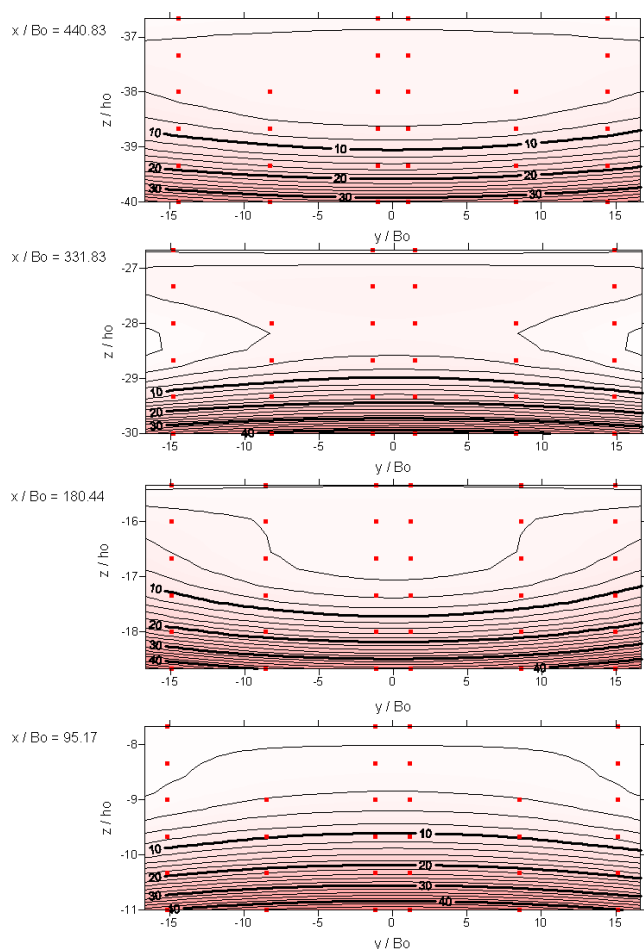


Fig. 21. Swell:  $H_s = 3.75$  cm,  $T_p = 1.5$  s,  $B_0 = 6$  cm,  $h_0 = 1.5$  cm.

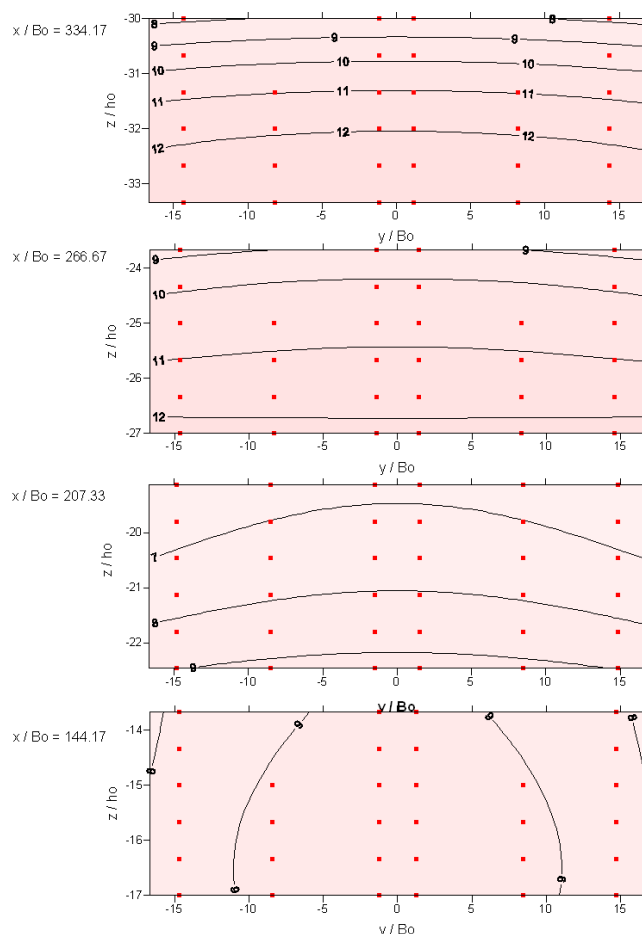


Fig. 22. Swell:  $H_s = 11.25$  cm,  $T_p = 2.5$  s,  $B_0 = 6$  cm,  $h_0 = 1.5$  cm.

Table 4

Progress velocity of the discharge. The positions are not the same, change from one test to another. The average is the slope from the regression line

Tests for this discharges conditions: $B_0 = 6$ cm; $h_0 = 1.5$ cm; $Q_0 = 23.4$ l/min	Progress velocity ( $uB_0h_0Q_0^{-1}$ )				
	Position 1	Position 2	Position 3	Position 4	Average
Calm: $H_s = 0$ cm, $T_p = 0$ s	0.203	0.086	0.108	0.123	0.105
Low swell: $H_s = 1.25$ cm, $T_p = 1$ s	0.122	0.087	0.118	0.122	0.109
Moderate swell: $H_s = 3.75$ cm, $T_p = 1.5$ s	0.073	0.112	0.122	0.115	0.116
Heavy swell: $H_s = 11.25$ cm, $T_p = 2.5$ s	0.043	0.020	0.021	0.058	0.032
Moderate swell regular: $H = 3.5$ cm, $T = 1.5$ s	—	—	—	—	0.116
Heavy swell regular: $H = 11.25$ cm, $T = 2.5$ s	—	—	—	—	0.049
Mixed swell regular: $H = 0$ cm, $T = 0$ s	—	—	—	—	0.114
$H = 3.5$ cm, $T = 1.5$ s	—	—	—	—	0.193

zone, it does easier to understand the reason because the dilution in moderate swell conditions is worst.

Other tests were performed now increasing the width discharge. Without going into the effects of this width increase in the dilution process and just appreciating

what the swell are concerned, it is observed that indeed, the same phenomenon happens again:

For swell that break within the plunged zone (calm conditions), the dilution decreases ( $D^{-1}(\%)$  increases, see Fig. 25) and reduces the plunged zone (Table 3). For swell

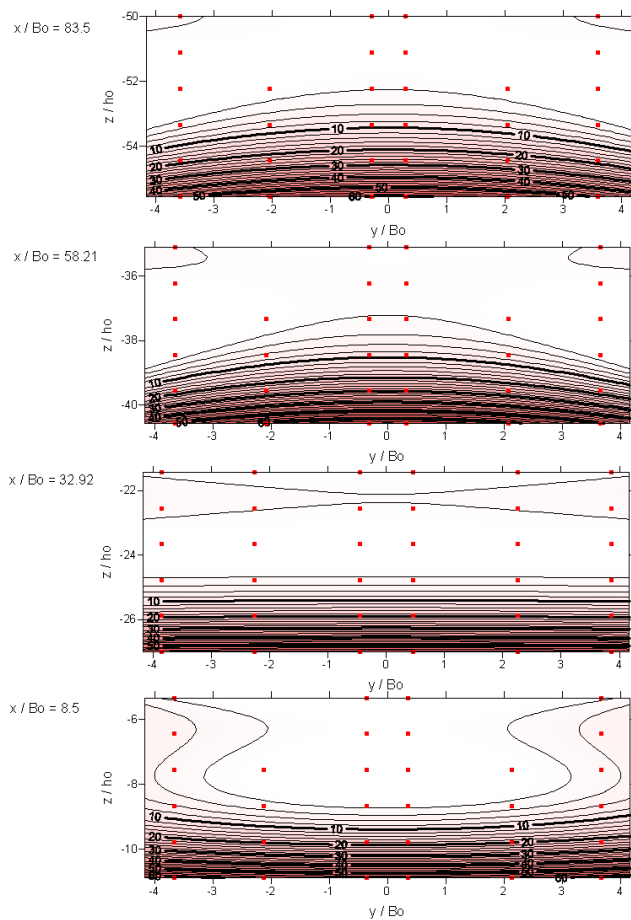


Fig. 23. Calm condition  $B_0 = 24$  cm,  $h_0 = 0.9$  cm.

that break outside the plunged zone of calm conditions, the dilution increases (the  $D^{-1}(\%)$  decreases) and the plunged zone increases with respect to calm conditions (see Figs. 23 and 24).

#### 4.2. Progress velocity and hyperdense layer velocity

During the tests the progress velocity of the discharge along the flume was also measured. The time in four different positions was measured (Pasteur pipettes position), except in the regular swell tests where the time was measured meter to meter.

The positions (Tables 4 and 5) for each test are different so it is not possible to compare the velocities between tests. However, it is interesting to observe the evolution of the magnitudes within each test.

It is observed that the velocity in Position 1 is the biggest in the remaining positions (except for moderate swell where Position 1 was away much from the discharge, Table 4). In Position 2 the velocity goes down and then, while the spill moves forward along the flume, it is accelerating without reaching steady state. In turn, it is observed that in the tests where there is a decrease of

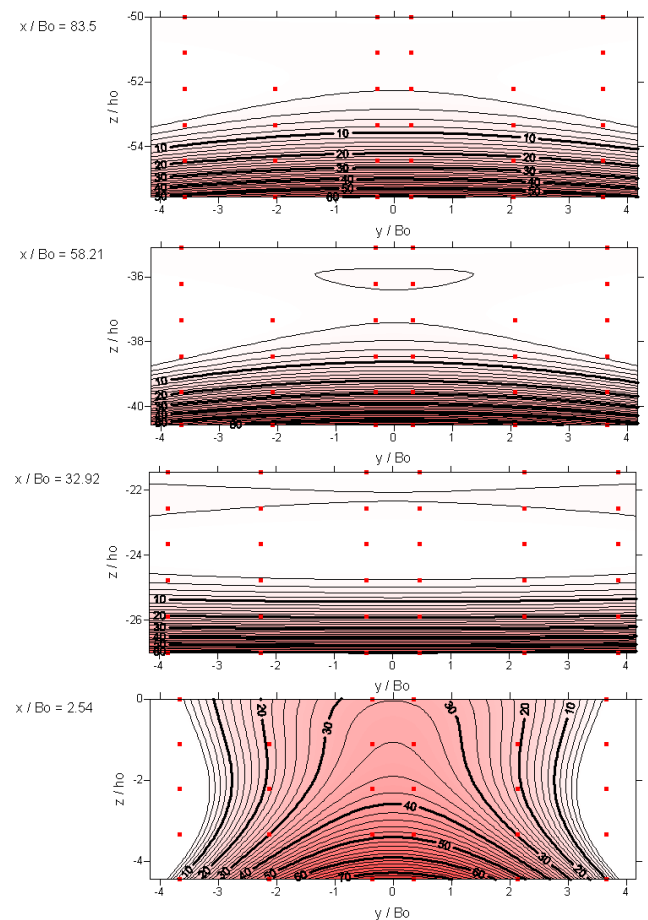


Fig. 24. Swell:  $H_s = 1.25$  cm,  $T_p = 1$  s,  $B_0 = 24$  cm,  $h_0 = 0.9$  cm.

dilution (Figs. 20 and 21) compared to calm conditions (Fig. 19), the average progress velocity is higher; and it is observed in those tests in where there is an increase of dilution, the average progress velocity is lower.

The hyperdense layer velocity was measured with the UPV in positions close to a set of tubes (Fig. 18 right). The results (Fig. 26) are consistent with anticipated by the theory [7]. There are positive and negative hyperdense layer velocities: the positive velocities mean a forward move of the hyperdense layer and the negative velocities mean a reverse move of the ambient. The positive velocities are placed at the bottom of the water column and show the velocity of the density current. While, the negative velocities are placed in the part of the water column above the hyperdense layer and show the velocity of the entrainment. The velocity zero shows the interface between discharge and environment.

The samples were collected for a moment within a test, so for irregular swell tests depend heavily of the moment that was chosen to sample and then the results present strong variations (Fig. 26 bottom). The figures show as the increases of swell conditions generate a decrease of hyperdense layer velocity. For low swell condition, there

Table 5

Progress velocity of the discharge. The positions are not the same, change from one test to another. The average is the slope from regression line

Tests for this discharges conditions: $B_0 = 24 \text{ cm}; h_0 = 0.9 \text{ cm}; Q_0 = 23.4 \text{ l/min}$	Progress velocity ( $uB_0h_0Q_0^{-1}$ )				
	Position 1	Position 2	Position 3	Position 4	Average
Calm: $H_s = 0 \text{ cm}, T_p = 0 \text{ s}$	0.353	0.254	0.271	0.283	0.271
Low swell: $H_s = 1.25 \text{ cm}, T_p = 1 \text{ s}$	0.813	0.260	0.271	0.283	0.272
Moderate swell: $H_s = 3.75 \text{ cm}, T_p = 1.5 \text{ s}$	0.542	0.181	0.232	0.253	0.213

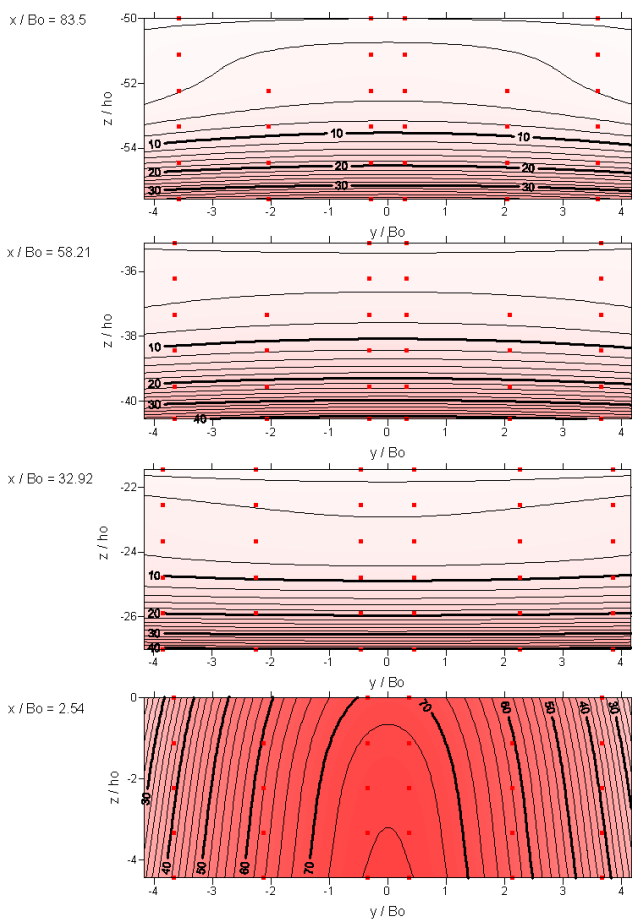


Fig. 25. Swell:  $H_s = 3.75 \text{ cm}, T_p = 1.5 \text{ s}, B_0 = 24 \text{ cm}, h_0 = 0.9 \text{ cm}$ .

is a small decrease in the velocity, but not significant, as in the salinity concentrations there are not many differences.

Changes are observed for the moderate swell. For example, the interface position is highly variable and depends on the moment when was sampled. Likewise, the velocities of bottom are highly variable, even hyperdense layer may take negative values, probably coinciding when the wave is very strong and stops the spill in plunged zone. These fluctuations will be analyzed further in the next section, when we analyze the results obtained

by the MSCTi. These fluctuations were called “evolution fronts” and were appearing throughout the entire test. These “evolution fronts” have a specific frequency of occurrence which depend on the irregular swell period and the accumulation of mass discharge in the surf zone.

### 4.3. Frequency analysis

In each test, the MSCTi was positioned next to a sample extraction pipette. The difference in measurement between the pipette and the MSCTi is that the pipette provides an average of salinity during 1 or 2 min, while the MSCTi provides a measurement each 0.05 s, providing a powerful tool to observe the temporal variability, such as swell which is determined by a certain period. Usually, the MSCTi was located in the bottom of the physical model, but in several tests was located a few millimetres away from the bottom trying to detect the “evolution front” totally.

Noting the figures, the average value in the  $D^{-1}(\%)$  is almost the same in the case of calm conditions (Fig. 27) and low swell conditions (Fig. 28). Not so in its temporal behaviour. While in the calm condition, no regular and little intense fluctuations are observed, in the case of low swell condition this fluctuations are more intense and with high frequency.

In the moderate swell condition (Fig. 29), magnitude and behaviour changes are perceived respect calm condition. The most significant change is the minimum  $D^{-1}(\%)$  that appears approximately every 4–4.5 min. If the generated wave train is analyzed, it has duration of 13.5 min; if this time is transferred to the graph, this period coincide every 13.5 min with the minimum, the maximum and the various oddities of the figure. Likewise if this same operation is performed in the Heavy swell Test (which wave train generated has duration of 21.75 min), it is observed that, from qualitative point of view, the peaks and valleys coincide fairly accurately each 21.75 min.

Given these singularities, some tests with regular swell were performed in search of certain parallels between the wave behaviour and changes in salt concentration. Figs. 31 and 32 represent the data obtained for a moderate ( $H = 3.5 \text{ cm}$  and  $T = 1.5 \text{ s}$ ) and heavy regular swell ( $H = 11.25 \text{ cm}$  and  $T = 2.5 \text{ s}$ ). Fig. 33 represents a mix-test,

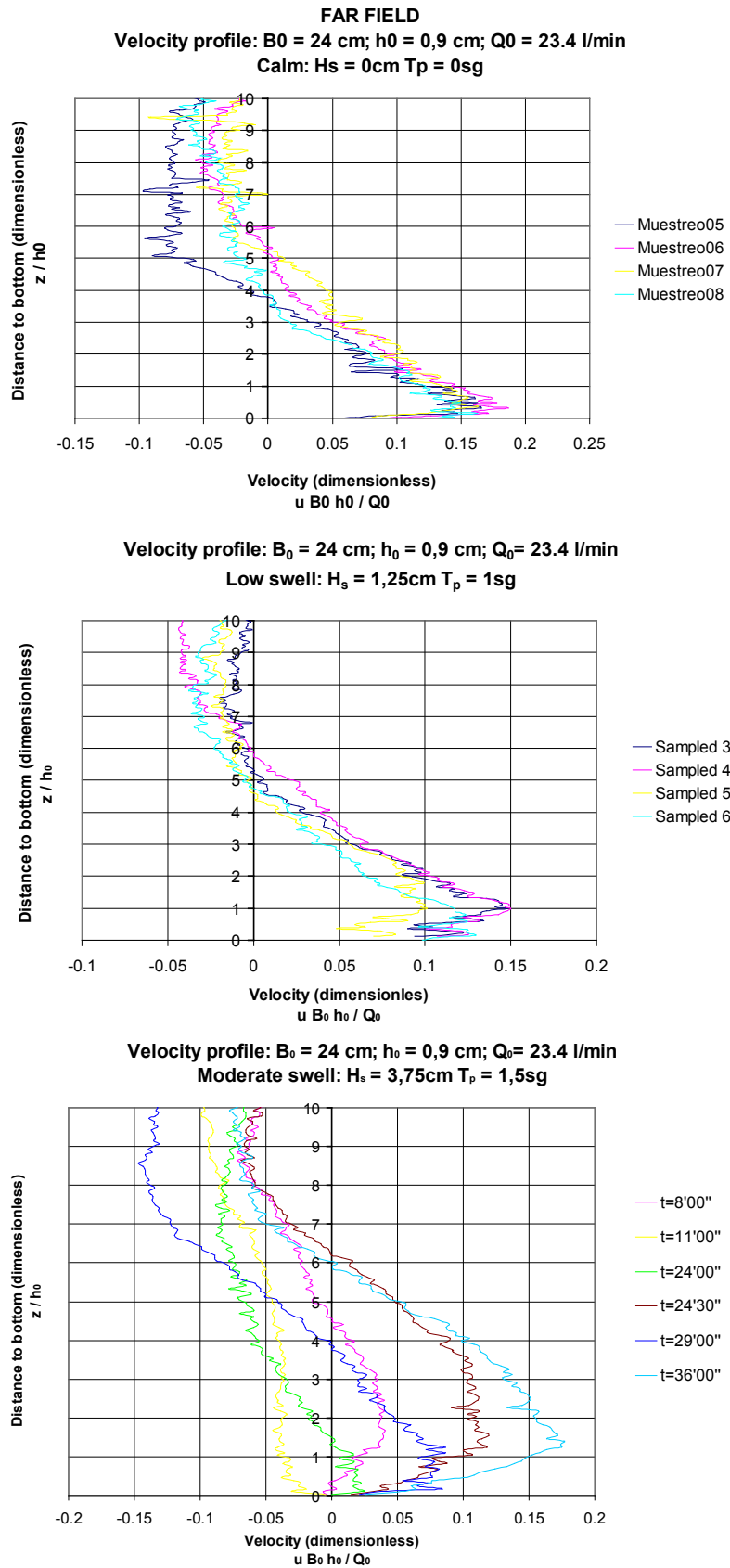


Fig. 26. Velocity profiles for different swell conditions.



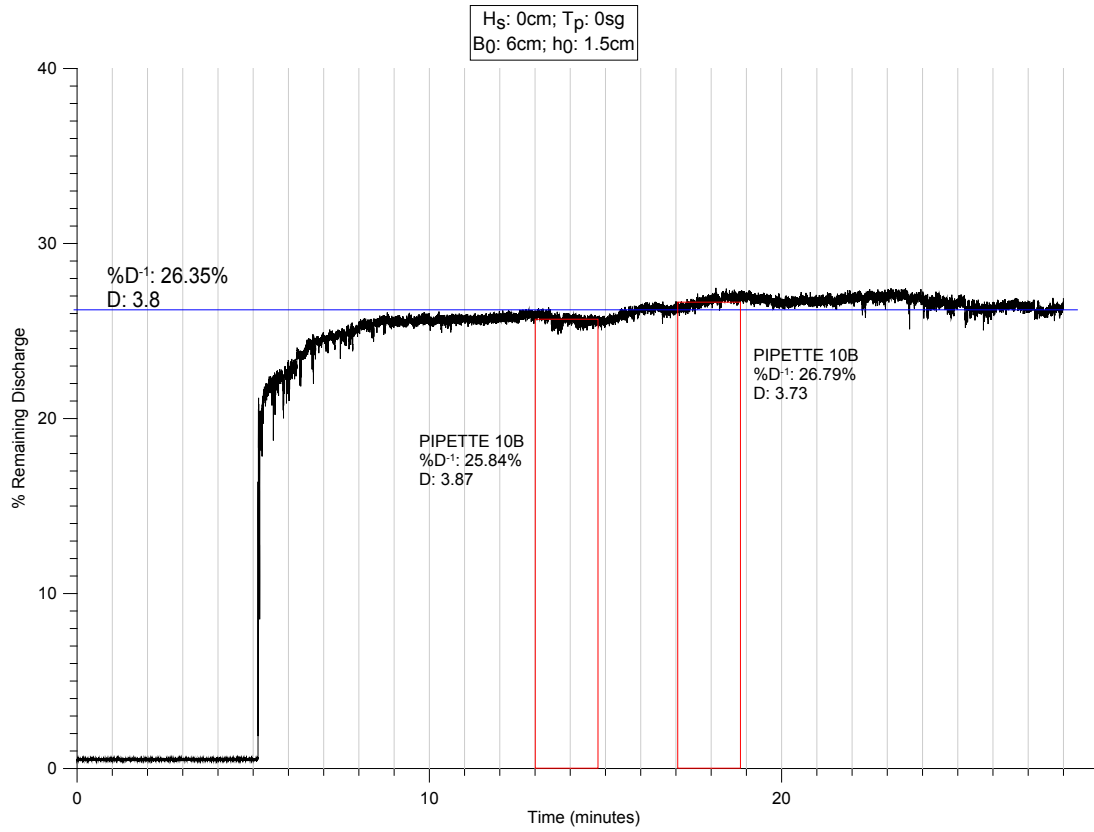


Fig. 27. Calm condition. Initial discharge:  $B_0 = 6$  cm;  $h_0 = 1.5$  cm.

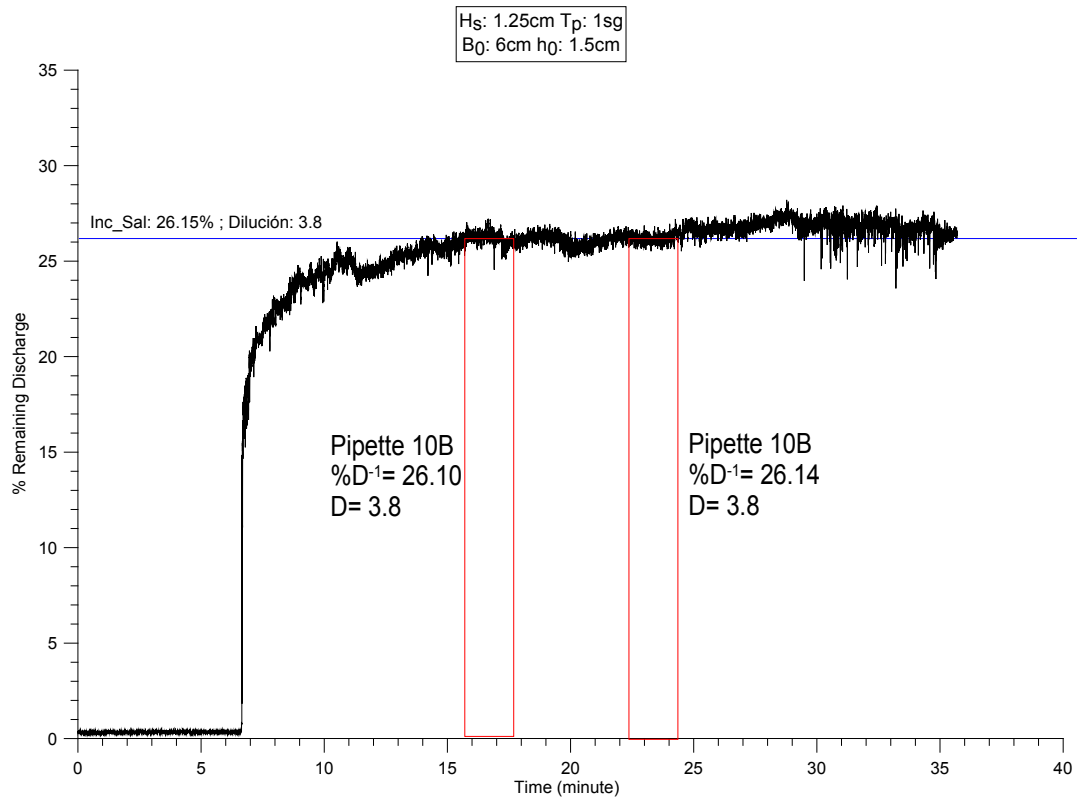


Fig. 28. Low swell.  $H_s = 1.25$  cm,  $T_p = 1$  s.. Initial discharge:  $B_0 = 6$  cm,  $h_0 = 1.5$  cm.

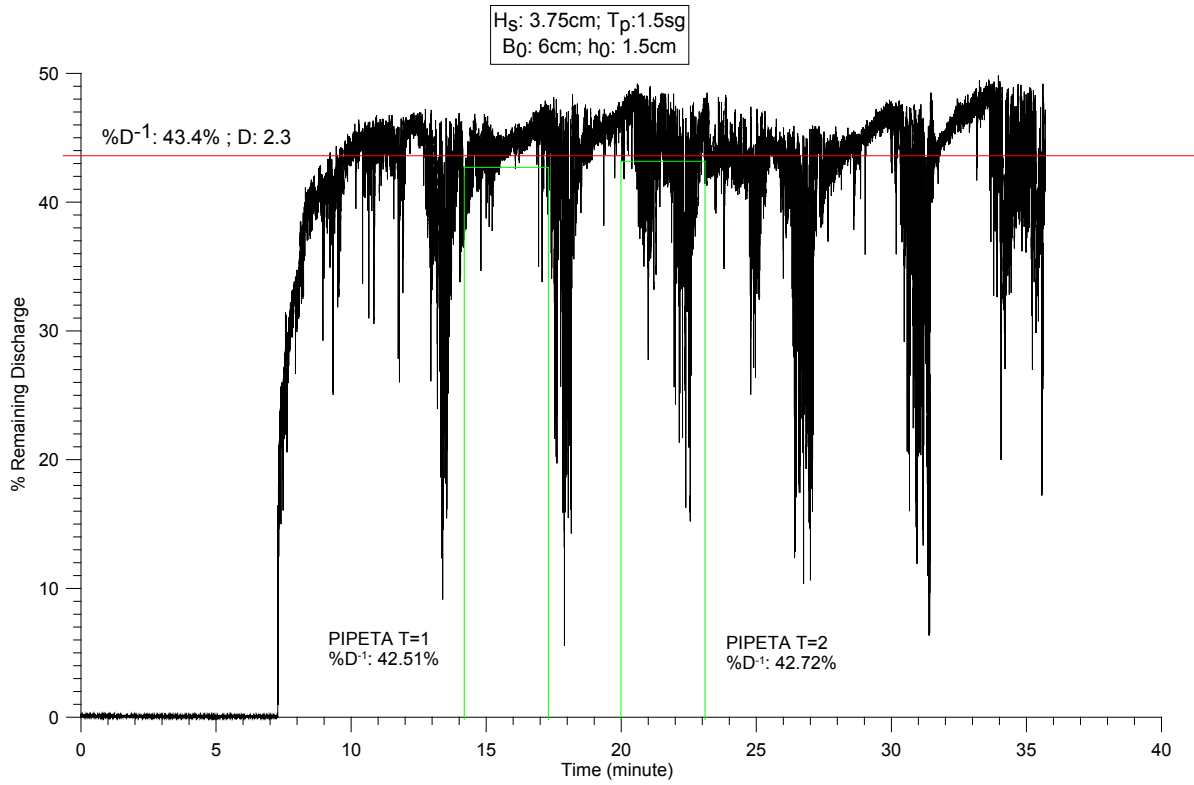


Fig. 29. Moderate swell.  $H_s = 3.75$  cm,  $T_p = 1.5$  s. Initial discharge:  $B_0 = 6$  cm,  $h_0 = 1.5$  cm.

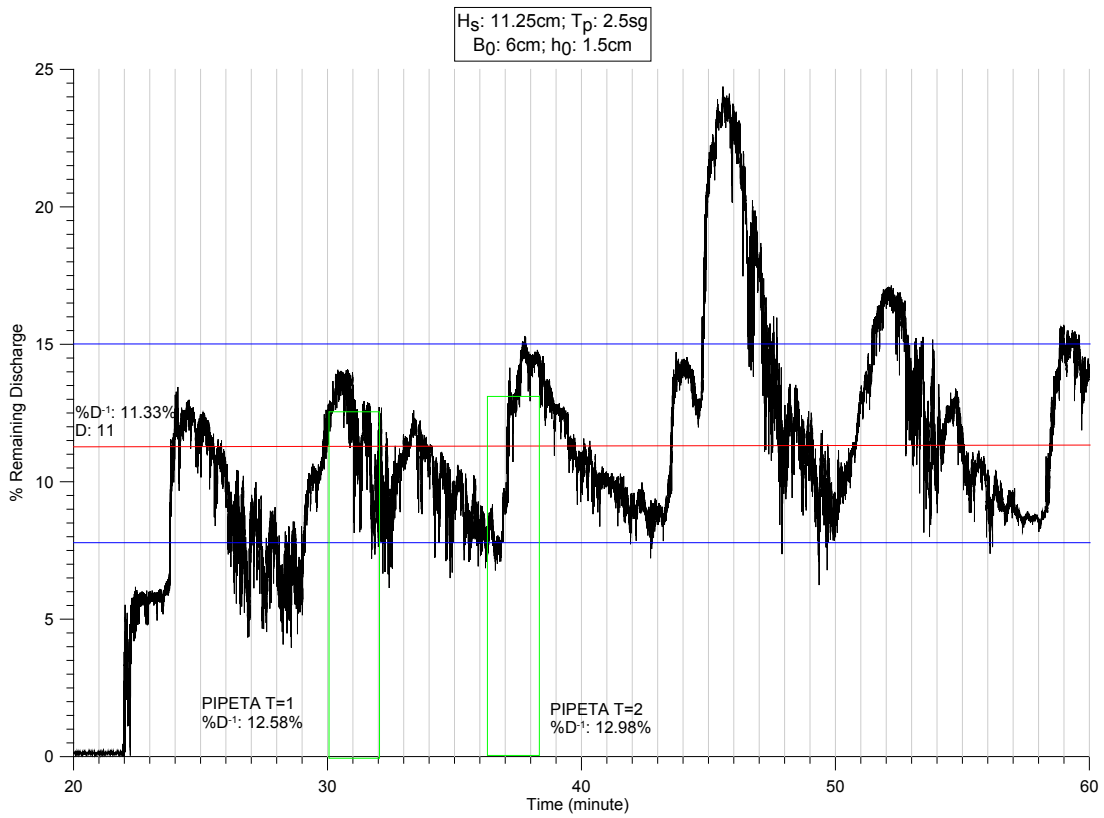


Fig. 30. Heavy swell.  $H_s = 11.25$  cm,  $T_p = 2.5$  s. Initial discharge:  $B_0 = 6$  cm,  $h_0 = 1.5$  cm.

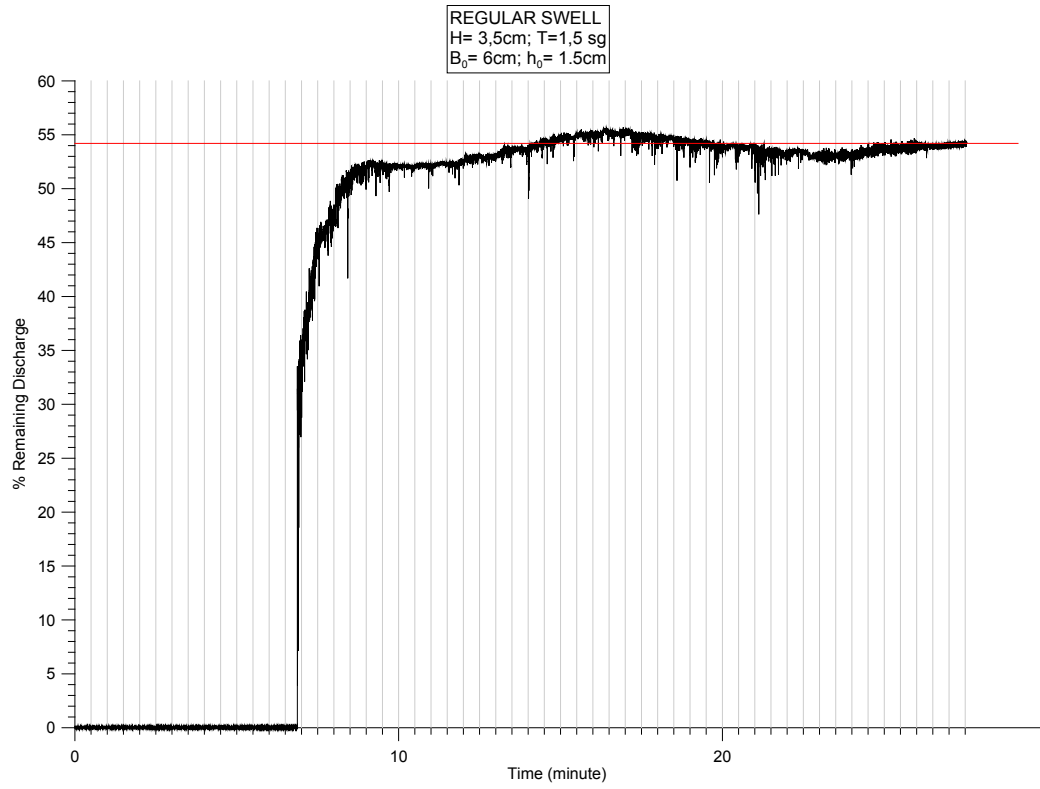


Fig. 31. Moderate regular swell.  $H = 3.5\text{ cm}$ ,  $T_p = 1.5\text{ s}$ . Initial discharge:  $B_0 = 6\text{ cm}$ ,  $h_0 = 1.5\text{ cm}$ .

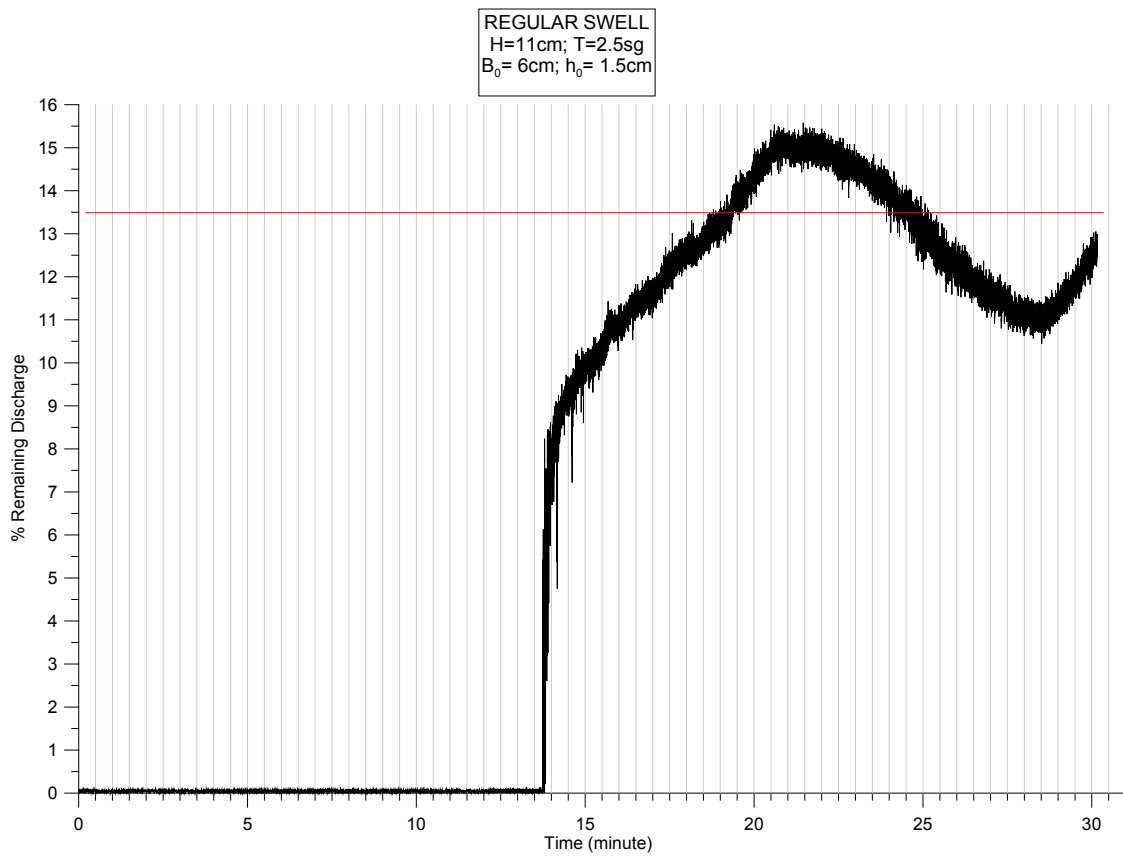


Fig. 32. Heavy regular swell.  $H = 11.25\text{ cm}$ ,  $T = 2.5\text{ s}$ . Initial discharge:  $B_0 = 6\text{ cm}$ ,  $h_0 = 1.5\text{ cm}$ .

which the first 16 min there were no waves, and after this time, a moderate regular swell was generated.

In Fig. 32 (heavy waves) a fluctuate is observed dramatically obvious and regular, the period is approximately 12.5 min, which in principle has no relationship with the waves generated ( $T = 2.5$  s). Also, according to Fig. 31 (moderate wave) there is a large fluctuation of 12.5 min, so probably this fluctuation is produced to the dimensions of the flume. Also, there are high-frequency fluctuations; these fluctuations were called “evolution fronts”. During the test, many “evolutionary fronts” were observed with a regular period. Very marked minimum peaks can be seen in Fig. 31 (can count to 10 per min). As the MSCTi was at the bottom, this minimum peaks are not so marked as in Fig. 29 (MSCTi was a few mm from the bottom), but they have greater regularity and duration.

Fig. 33 (mixed swell test) shows clearly the decrease in dilution that the swell produce. In turn, although the swell started in the 16th min, any change is not observed until the 21st min. This implies that dilution happens practically in the plunged zone (surf zone). That time elapsed between 16th and 21st min is the time it took to

release their new conditions to reach the position of the MSCTi. During these five minutes no change in the signal is observed. So, what is measured during those 5 min is the diluted discharge in the plunged zone which is coming to MSCTi with no increase or decrease in the dilution.

To quantify these measures, FFT (fast Fourier transform) analyses of the signal were performed. Previously, the series with no recorded data were erased and in turn two filters used (low pass – high pass), one for low frequencies and one for high frequencies (Fig. 34).

The results of FFT analysis are presented in Table 6.

The period of 12.5 min visually in Figs. 31 and 32 is not observed because there is only one cycle. Moreover, in the moderate swell, the FFT results at high frequencies are closed to the peak periods of the swell. Also, it is observed that the low-frequencies are those with the biggest energy, principally it is observed in the FFT where was performed with full signal. According to the observations, the low-frequency results correspond to the visual shape of the signal (peaks and valleys) and high-frequencies are related to the period of the swell.

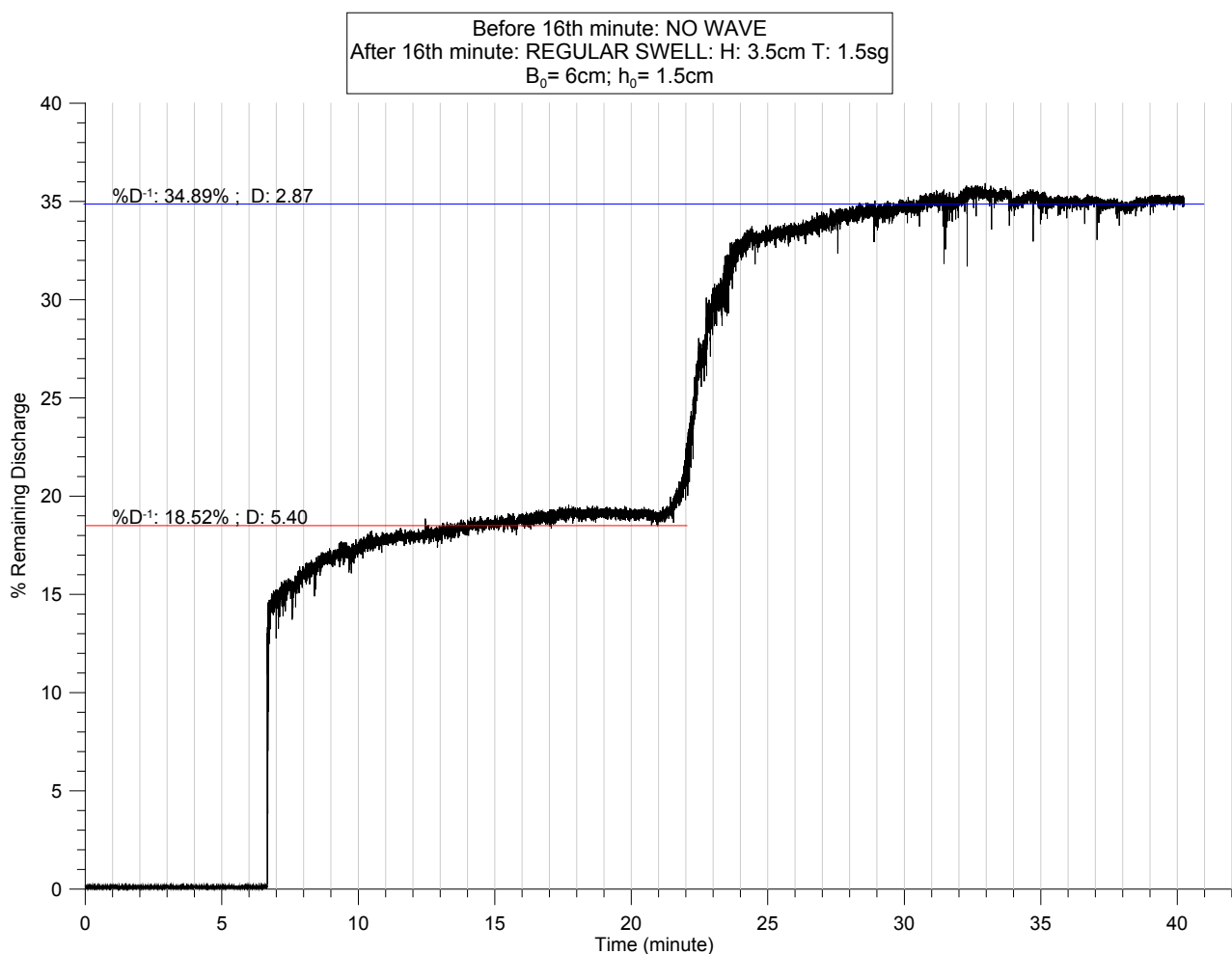


Fig. 33. Mixed swell: first 16 min: calm condition. After the 16th min: regular moderate swell.  $H = 3.5$  cm,  $T = 1.5$  s. Initial discharge:  $B_0 = 6$  cm,  $h_0 = 1.5$  cm.

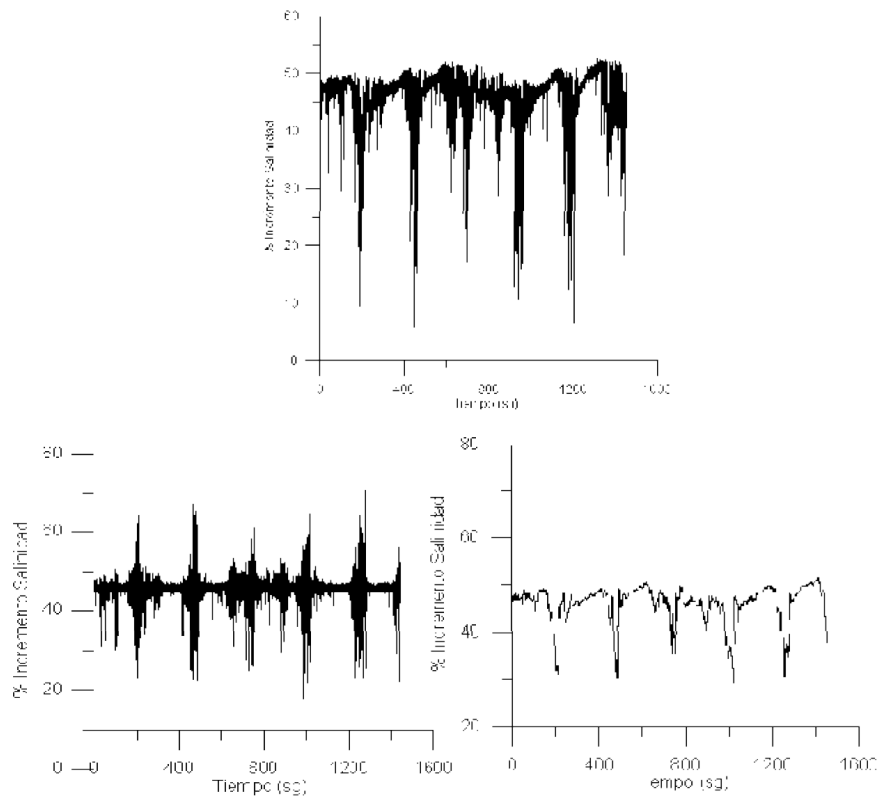


Fig. 34. Example of filtered time series. Top: unfiltered signal, bottom left: higher frequencies, bottom right: low frequencies.

Table 6  
Result of frequency analysis

	Complete signal period*	High-frequency period*	Low-frequency period*
Moderate swell: $H_s = 3.75$ cm, $T_p = 1.5$ s	192.6 s = 3.20 min	9 s 1.66 s	154.05 s = 2.57 min
Heavy swell: $H_s = 11.25$ cm, $T_p = 2.5$ s	468 s = 7.8 min	1.93 s	315.8 s = 5.26 min
Regular moderate swell: $H = 3.5$ cm, $T = 1.5$ s	207 s = 3.45 min 171.5 s = 2.86 min	0.41 s 1.5 s	258.7 s = 4.29 min 36.2 s
Regular heavy swell: $H = 11.25$ cm, $T = 2.5$ s	194.6 s = 3.24 min	1.26 s	161.42 s = 2.7 min

\*Secondary periods are indicated by having a very similar magnitude to the principal

**5. Conclusions**

1. The wave variable is essential when analyzing the surface discharges of the desalination plants.
2. A lack of ruling out the effects of the narrow of the test flume, it can be concluded that if the incident wave breaks, mostly, in the plunged area that it would have in calm conditions, it will cause a significant decrease dilution.
3. In turn, with the same flow discharge, the dilution is highly dependent on the width of the discharge. This produces a significant deterioration with increasing the width (Figs. 19 and 23).
4. The maximum mixing occurs in the plunged zone. Once that the discharge is sunk and the hyperdense layer is formed, the dilution varies slowly in the longitudinal of the discharge.
5. According to the type of the wave (regular or irregular) or their period, it forms the “evolution fronts” which gets wider the hyperdense layer due to a compression of the discharge in the plunged zone because of the tensor wave radiation.
6. The evolution fronts do not imply an instantaneous increase of salinity at the bottom, but it only implies that the hyperdense layer gets wider.
7. Velocity progress of the hyperdense layer varies sig-

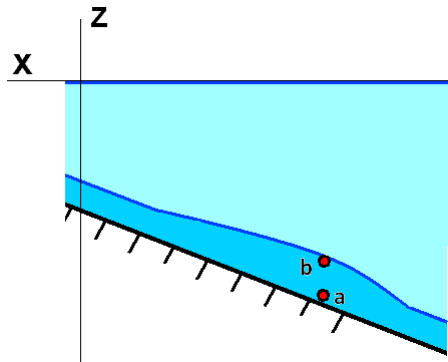


Fig. 35. Front of evolution through a sampling point of the MSCi. The point “a” corresponds to Fig. 28. The point “b” corresponds to Figs. 29, 31, 32.

nificantly with wave train that is coming in that instant and, in turn, with the wave train that is formed by the mixture in the plunged zone (surf zone).

### Symbols

$A$	— Section cross flow
$B_0$	— Flow width at inlet
$C$	— Conductivity, mS/cm
$D$	— Dilution = $Q/Q_0$
$D^{-1}(\%)$	— Percentage of remaining discharge = $100 \cdot D^{-1}$
$e_0$	— Flow thickness (depth) at inlet
$F_{d,B0}$	— Densimetric Froude number based on width at inlet
$F_{d,h0}$	— Densimetric Froude number based on thickness at inlet
$G_0$	— Buoyancy flux = $g'Q_0$
$g'$	— Reduction of gravitational acceleration = $g_0 \cdot \Delta \rho \cdot \rho_0^{-1}$
$H$	— Wave height (regular swell)
$H_s$	— Wave significant height for an irregular wave train
$L_{QM}, L_{QG}, L_{MG}$	— Scale length
$M_0$	— Momentum flux = $u_0 Q_0$
$Q$	— Flow at anyplace (entrainment + $Q_0$ )
$Q_0$	— Flow rate
$S$	— Salinity, psu
$T^\circ$	— Temperature

$T$	— Period (regular swell)
$T_p$	— Peak period for an irregular wave train
$u_0$	— Inflow velocity
$\rho_0$	— Discharge density
$\Delta \rho$	— Density difference between density current and ambient = $\rho_0 - \rho_a$

### References

- [1] A. Ruiz-Mateo and J. Martínez, Desalination and the environment, Desalination in Spain, Chap. 5. Ministerio Medio Ambiente, 2008.
- [2] J. Sánchez Lizaso, J. Romero, J. Ruiz, E. Gacia, J. Buceta, O. Invers, Y. Fernández, J. Mas, A. Ruiz-Mateo and M. Manzanera, Salinity tolerance of the Mediterranean seagrass *Posidonia oceanica*: recommendations to minimize the impact of brine discharges from desalination plants, *Desalination*, 221 (2008) 602–607.
- [3] Water Desalting Planning Guide for Water Utilities, Water Desalting Committee of the American Water Works Association, Wiley, 2004.
- [4] Centre for Studies on Ports and Coast, Research on discharge into the sea of rejection water from desalination plants. Final report, CEDEX Technical Report 23-500-7-005, 2003 (in Spanish).
- [5] Centre for Studies on Ports and Coast, Study of the dispersion of discharge into the sea through a dry riverbed of rejection water from a seawater desalination plant of Alicante Channel. Final report, CEDEX Technical Report 23-401-6-002, 2002 (in Spanish).
- [6] P. Palomar, A. Ruiz-Mateo, I.J. Losada, J.L. Lara, A. Lloret, S. Castanedo, A. Álvarez, F. Méndez, F. Rodrigo, P. Camus, F. Vila, P. Lomónaco and M. Antequera, MEDVSA: a methodology for design of brine discharges into seawater, *Desal. Wat. Reuse*, 20/1 (2010) 21–25.
- [7] V. Alavian, G.H. Jirka, R.A. Denton, M.C. Johnson and G.C. Stefan, Density currents entering lakes and reservoirs. *J. Hydraulic Eng.*, 118(11) (1992) 1464–1489.
- [8] J. Akiyama and H.G. Stefan, Plunging flow into a reservoir: Theory. *J. Hydraulic Eng.*, 110 (1984) 484–499.
- [9] T.R. Johnson, C.R. Ellis and H.G. Stefan, Negatively buoyant flow in a diverging channel. IV. Entrainment and dilution. *J. Hydraulic Eng.*, 115(4) (1989) 437–456.
- [10] A. Ruiz-Mateo, M. Antequera and J. Gonzalez, Physical modeling of brine discharges to the sea, *MWWD*, 2008.
- [11] M.D. Miles and D. Pelletier, User guide for GEDAP wave generation software: Update to Windows NT4/Windows 2000 Version, Canadian Hydraulic Centre Laboratory Memorandum, 2001.
- [12] M. Arita, M. Nakai and J. Umemoto, Flow and spreading of three-dimensional negatively buoyant surface jets discharged on a sloping bottom. 5th Int. Symp. on Stratified Flows, Vancouver, 2000.
- [13] A. Purnama and H. Al-Barwani, Modelling dispersion of brine waste discharges from a coastal desalination plant. *Desalination*, 155 (2003) 41–47.